

# Superconductivity in the noncentrosymmetric $\text{Li}_2\text{Pd}_{3-x}\text{Ag}_x\text{B}$ with $x=0.0, 0.1$ and $0.3$

A.A. Castro · O. Olicón · F. Morales · R. Escudero

Received: date / Accepted: date

**Abstract** We studied the partial substitution of Ag in the noncentrosymmetric superconducting compounds  $\text{Li}_2\text{Pd}_{3-x}\text{Ag}_x\text{B}$  with  $x=0.0, 0.1$  and  $0.3$ . Magnetization, resistivity and specific heat measurements were performed in this system. From electrical measurements we obtained the critical temperature  $T_c$ . The upper critical field at zero temperature was determined with Werthamer-Helfand equation,  $\mu_0 H_{c2}^{WHH}(0)$ , and  $\mu_0 H_{c2}^{linear}(0)$  and the coherence length,  $\xi(0)$ . The Value of  $\mu_0 H_{c2}^{linear}(0)$  and  $\mu_0 H_{c2}^{WHH}(0)$  is lower than the calculated paramagnetic Pauli limit suggesting that the spin-triplet pairing is weak in the system. From specific heat measurements we obtained the parameters of the normal state; the Sommerfeld coefficient,  $\gamma$ , the electronic density of states at the Fermi level,  $N(E_F)$  and the Debye temperature,  $\theta_D$ . In the superconducting state the obtained values were;  $\Delta C/\gamma T_c$ , the electron phonon coupling,  $\lambda_{e-ph}$ , the superconducting energy gap,  $2\Delta_0$ , and the ratio  $2\Delta_0/k_B T_c$ . The electronic specific heat is well described by the BCS theory, suggesting that the energy gap is isotropic and in a strong coupling state.

**Keywords** Superconductivity, Noncentrosymmetric, Specific heat

## 1 Introduction

Since the discovery of superconductivity in 1911, the search for novel superconductors specially materials with

higher critical temperatures have been carried out intensively. Superconducting materials can be classified in many categories: metal-based system, copper-oxygen, and iron pnictides/chalcogenides (iron-based superconductors), and others [1].

For instances, Iron-based superconductors are ideal candidates for several applications of superconductivity: wires, tapes, and coated conductors for high magnetic fields. The polycrystalline compound FeSe, is an interesting material for bulk applications like superconducting trapped-field magnets or super-magnets [2,3,4].

Superconductivity in materials without inversion symmetry exhibit engaging properties because a strong modification of the electronic band structure caused by antisymmetric spin-orbit coupling ASOC [5]. It has been shown that ASOC acts unfavorable on spin-triplet pairing states [6]. For spin single states the influence of ASOC is minor. The presence of ASOC leads to a splitting of the electronic bands by lifting the spin degeneracy and consequently splitting the Fermi surface. In noncentrosymmetric superconductors the two electronic bands forming Cooper pairs belong to two different Fermi surface corresponding to the spin-up and spin-down bands [7]. The presence, or absence of inversion symmetry may leads to a mixture of spin-singlet and spin-triplet coupling [7,8,9,10,11]. Depending on the type of the pairing interactions, the gap function may be characterized by the presence of line nodes [9].

Noncentrosymmetric heavy fermion superconductors such as  $\text{CeRhSi}_3$  [12],  $\text{CeIrSi}_3$  [13],  $\text{UIr}$  [14],  $\text{CePt}_3\text{Si}$  [15, 16] have attracted attention because the unconventional behavior in these strongly correlated electronic compounds. On the other side, transition-metal compounds like  $\text{Li}_2\text{Pd}_3\text{B}$  [17],  $\text{Li}_2\text{Pd}_{3-x}\text{Cu}_x\text{B}$  with  $x=0.0, 0.1$  and  $0.3$  [18],  $\text{Li}_2\text{Pt}_3\text{B}$  [19],  $\text{Mg}_{10}\text{Ir}_{19}\text{B}_{16}$  [20],  $\text{Rh}_2\text{Ga}_9$ ,  $\text{Ir}_2\text{Ga}_9$

---

A.A. Castro · O. Olicón · F. Morales · R. Escudero  
 Instituto de Investigaciones en Materiales, Universidad Nacional Autónoma de México, Ciudad de México, 04510, México.  
 E-mail: aacastroespinosa@gmail.com

[21],  $\text{Nb}_{0.18}\text{Re}_{0.82}$  [22] are more suitable for exploring the issue of inversion symmetry breaking. In previous reports, the ternary metallic borides  $\text{Li}_2\text{Pd}_3\text{B}$  were classified as noncentrosymmetric conventional superconductor without strong electronic correlation [17, 23, 24].

One antecedent different to this issue is that the well known ternary metallic boride  $\text{Li}_2\text{Pd}_3\text{B}$ , discovered by Togano with transition temperature about 8 K [17], was classified as noncentrosymmetric conventional superconductor without strong electronic correlation [23, 24].

In this study we present the effect of substitution of Pd with a nonmagnetic element, in an early reported [18]. We choose the substitution of Pd with Ag, a non magnetic element. The reason was because is isostructural and the atomic ratio of Ag is bigger than Pd. The difference in the atomic ratio should generates a internal pressure effect in the unit cell and modify the superconducting properties. In this work we study the characteristics of this compound: crystalline structure, magnetic and electronic specific heat  $\text{Li}_2\text{Pd}_{3-x}\text{Ag}_x\text{B}$  with three Ag compositions;  $x=0.0, 0.1$  and  $0.3$ . We compare and observe the Pauli limit with the upper critical field because is a criterion related to the importance of the spin-triplet piring component. We estimate the parameters of the normal and superconducting state, and the strength of the electron-phonon coupling.

## 2 Experimental details

Polycrystalline samples of  $\text{Li}_2\text{Pd}_{3-x}\text{Ag}_x\text{B}$  with three compositions;  $x=0.0, 0.1$  and  $0.3$  were synthesized by two steps in an arc-melting apparatus in order to minimize losses of Li by evaporation. Stoichiometric samples were prepared using 20% of Li (99 +%), Pd (99.95%), Ag (99.95%) and B (99.99%) powders as precursors. The melting was performed in a chamber with high pure argon atmosphere. X ray diffraction patterns were measured at room temperature in a Siemens (D5000) diffractometer with  $\text{Co } K_\alpha$  radiation ( $\lambda=1.79026 \text{ \AA}$ ) and Fe filter in steps of  $.015^\circ$  at 8 s in the  $2\theta$  range of  $20^\circ$ - $110^\circ$ . Rietveld analysis of the diffraction patterns were performed with MAUD program [25].

Electrical resistance versus temperature  $R(T)$  and magnetic field were measured in a Physical Properties Measurement System, PPMS (Quantum Design).  $R(T)$  without magnetic field were measured from 300 K to 2 K. The magnetoresistance measurements were determined between 2 K and 10 K with applied magnetic field between 0 and 40 kOe. Magnetization measurements were determined in a MPMS magnetometer (Quantum Design). Temperature dependence of the magnetic susceptibilities were investigated under zero field cooling (ZFC) and field cooling (FC) modes.

Specific heat measurements were determined using a relaxation method between room temperature and 2 K in the PPMS system. The sample was attached to the measuring stage using Apiezon N grease to ensure a good thermal contact. The contribution to the heat capacity of the sample holder and grease was subtracted from the sample measurements.

## 3 Results and discussion

### 3.1 Structural characterization

X-ray diffraction patterns for the polycrystalline samples  $\text{Li}_2\text{Pd}_{3-x}\text{Ag}_x\text{B}$  with the three compositions:  $x=0.0, 0.1$  and  $0.3$  are shown in Figure 1. The main features of the patterns correspond to a cubic structure  $P4_332$ . A small amount of impurities  $\text{Pd}_2\text{B}_5$  (\*) and  $\text{PdB}_2$  (+) were detected. It is worth mentioning that  $\text{PdB}_2$  is non-superconducting [26].

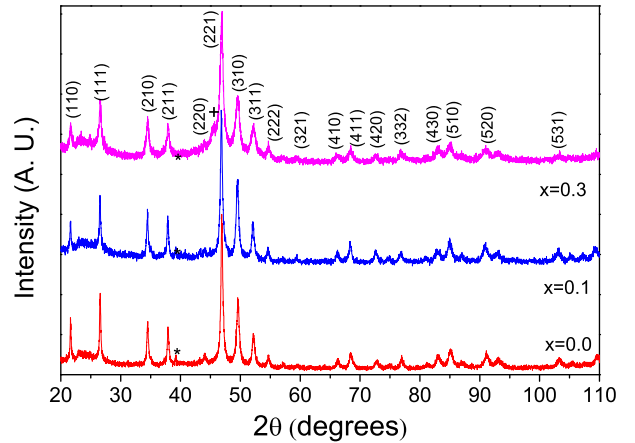


**Fig. 1** X-ray diffraction patterns for  $\text{Li}_2\text{Pd}_{3-x}\text{Ag}_x\text{B}$  with  $x=0, 0.1$  and  $0.3$ . The reflections observed at  $39.3^\circ$  correspond to a tiny impurity of  $\text{Pd}_2\text{B}_5$  and  $\text{PdB}_2$  respectively.

The X-Ray diffraction patterns were Rietveld-fitted considering the possibility that Ag ions can occupy Pd sites. Figure 2 shows the refined pattern of  $\text{Li}_2\text{Pd}_{2.9}\text{Ag}_{0.1}\text{B}$  sample. Vertical lines, at the bottom of the panel are the reported reflections (ICSD 84931), the Miller indexes of each plane are indicated.

The structural parameters and R-factors are summarized in Table 1. The structural parameters and R-factors obtained from the Rietveld analysis, for the three samples in study, shows increase of the lattice parameter,  $a$ , as the nominal concentration of Ag increases. This results from the atomic radius difference between Pd ( $1.28\text{\AA}$ ) and Ag ( $1.34\text{\AA}$ ). This certainly suggests

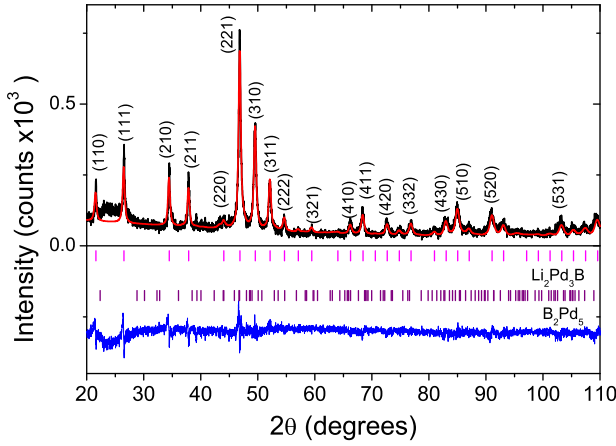


**Fig. 2** Rietveld results for the  $\text{Li}_2\text{Pd}_{2.8}\text{Ag}_{0.1}\text{B}$  sample along with experimental (black line) and calculated pattern (red line). Vertical lines are the reflections of  $\text{Li}_2\text{Pd}_3\text{B}$  and  $\text{Pd}_2\text{B}_5$ . The line at the bottom is the difference between experimental and refined pattern

that Ag has substituted Pd in the  $\text{Li}_2\text{Pd}_{3-x}\text{Ag}_x\text{B}$  with  $x=0.0, 0.1$  and  $0.3$  system. At concentrations  $x>0.3$  traces of Ag were detected, so we considered just  $x=0.0, 0.1$  and  $0.3$ .

**Table 1** Structural parameters obtained from the Rietveld fitting of the X-ray diffraction patterns of the studied compound with Ag at 295 K.

	$x=0.0$	$x=0.1$	$x=0.3$
$a$ (Å)	6.7427(3)	6.7548(3)	6.7637(9)
$V$ (Å <sup>3</sup> )	306.6	308.2	309.4
$R_w$ (%)	15.82	16.28	14.34
$R_b$ (%)	12.28	12.72	11.08
$R_{exp}$ (%)	10.87	11.98	10.37
$\chi^2$ (%)	1.45	1.35	1.38
$\text{Li}_2\text{Pd}_{3-x}\text{Ag}_x\text{B}$ (%)	90.5590	97.5043	80.1257
$\text{B}_2\text{Pd}_5$ (%)	9.4490	2.4956	19.0506
$\text{Pd}_2\text{B}$ (%)	-	-	0.8235

### 3.2 Magnetic and electrical measurements

Magnetization curves in zero-field-cooling (ZFC) and field-cooling (FC) modes as function of temperature under 20 Oe applied magnetic field are shown in Figure 3. A drop of magnetization below 8 K was observed for the samples in this work. The critical temperature,  $T_c$ , was determined as the onset of the transition. The superconducting transition decreases gradually with doping of Ag. The samples in studied present a low fraction corresponding to the Meissner effect (FC) comparable to the shielding effect (FC) which is common to see in bulk polycrystalline metallic superconductors [17,19].

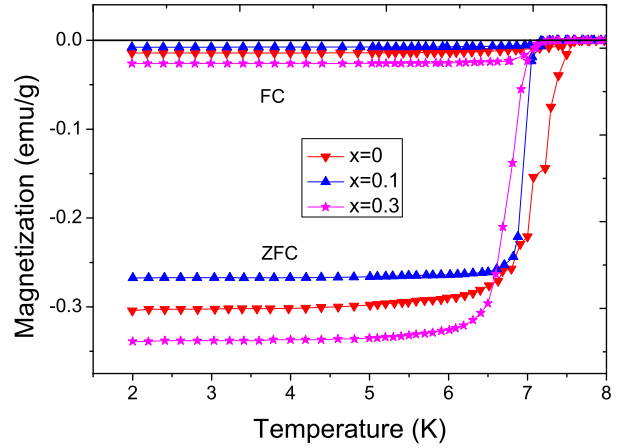


**Fig. 3** Magnetization as a function of temperature of  $\text{Li}_2\text{Pd}_{3-x}\text{Ag}_x\text{B}$  at constant magnetic field of 20 Oe.

The electrical resistance as a function of temperature  $R(T)$  from 2 to 300 K of the parent compound,  $\text{Li}_2\text{Pd}_3\text{B}$  is shown in Figure 4. The resistance shows a small decreasing behavior below room temperature. The residual resistance ratio ( $RRR = R_{300K}/R_{8K}$ ) is indicated. The  $RRR$  values provide a qualitative information about electron scattering by impurities and vacancies. For the samples studied the  $RRR$  values were 1.5, 3.0 and 2.9 for the three compositions ( $x=0.0, 0.1$  and  $0.3$ ) those values are in the range of 1.4 to 6.5 of the reported values for  $\text{Li}_2\text{Pd}_3\text{B}$  [23,17]. The small value of  $RRR$  obtained in this study could suggests that the normal-state resistivity has a weak temperature dependence on the electrical transport and very sensitive to impurities and disorder.

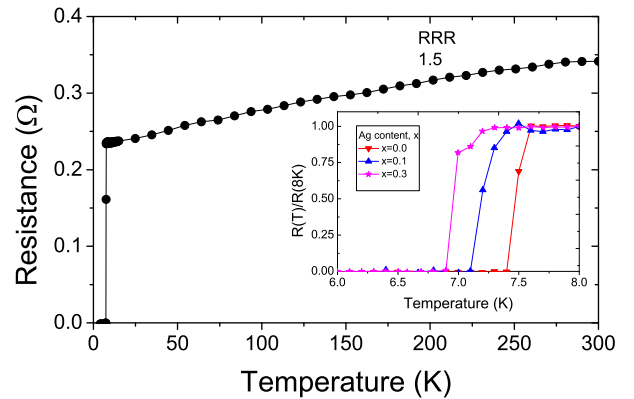


**Fig. 4** Resistance vs Temperature of  $\text{Li}_2\text{Pd}_3\text{B}$ , the residual resistance ratio ( $RRR$ ) of this sample is 1.5. The inset shows the normalized resistance  $R(T)/R(8K)$  curves above 2 K and up to 8 K, close to the superconductor transition, of the measured samples

The inset of figure 4 shows the normalized resistance with resistance value at 8 K. The superconducting transitions are sharp with a transition width of 0.21 K for the samples under study. The critical temperature was determined in the point at which the first derivative of the  $R(T)$  curve reaches its maximum value. The  $T_c$  values are 7.51 K, 7.19 K and 6.99 K for samples with  $x=0.0$ , 0.1 and 0.3 respectively. It can be seen that  $T_c$  decreases as the Ag content increases.

The resistance as function of temperature and magnetic field for the three studied samples in the 2-8 K temperature range under 0-4 T magnetic field is shown in Figure 5. The transition to the superconducting state is shifting to lower temperatures under the increase of DC magnetic field. From this curves we extracted the variation of the  $T_c$  with the applied field shown in Figure 6. The extrapolation of the linear fit of data the upper critical field at  $T = 0$  K,  $H_{c2}^{linear}(0)$ , with values of  $6.0 \pm 0.3$ ,  $5.2 \pm 0.1$  and  $5.1 \pm 0.1$  for the three samples.

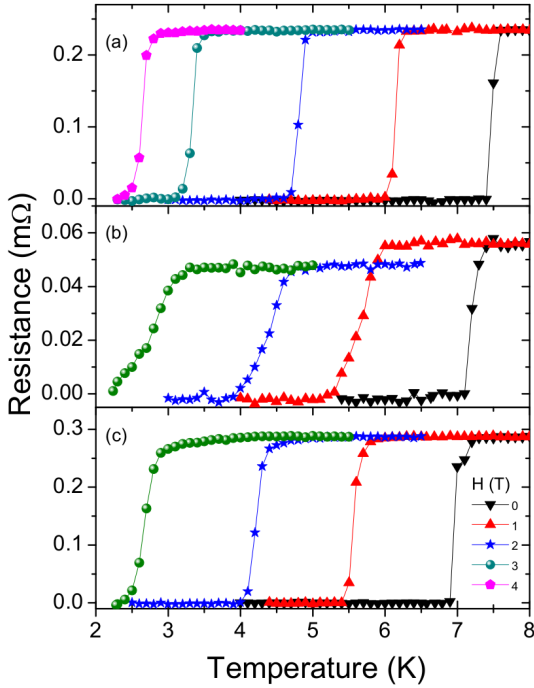


**Fig. 5** Magneto-resistance measurements with temperature and magnetic field for  $\text{Li}_2\text{Pd}_{3-x}\text{Ag}_x\text{B}$  (a)  $x=0.0$ , (b)  $x=0.1$  and (c)  $x=0.3$ . The symbols indicate the applied magnetic fields for the three samples.

The upper critical field at 0 K was estimated using the Werthamer-Halfand-Hohenberg theory [27]:

$$H_{c2}^{WHH}(0) = 0.693T_c \left( \frac{dH_{c2}}{dT} \right)_{T=T_c}, \quad (1)$$

this theory has been employed in several studies of noncentrosymmetric superconducting systems [18, 19, 20, 22, 23, 28].

The values of  $\mu_0 H_{c2}^{WHH}(0)$  obtained are 4.95 T, 4.43 T and 4.29 T for  $x=0.0$ , 0.1 and 0.3 respectively. The value of  $\mu_0 H_{c2}^{WHH}(0)$  (4.95 T) for the sample  $\text{Li}_2\text{Pd}_3\text{B}$  is comparable with the reported value of 4.8 T [17]. From the  $\mu_0 H_{c2}^{WHH}(0)$  values we calculate the coherence length,  $\xi(0)$ , using the Ginzburg-Landau equation:

$$H_{c2}(0) = \frac{\Phi_0}{2\pi\xi_0^2}, \quad (2)$$

where  $\Phi_0 = 2.0678 \times 10^{-15}$  T m<sup>2</sup> is the magnetic flux quantum. The values of  $\xi_0$  are 8.17, 8.64 and 8.78 nm for  $x=0.0$ , 0.1 and 0.3, respectively.

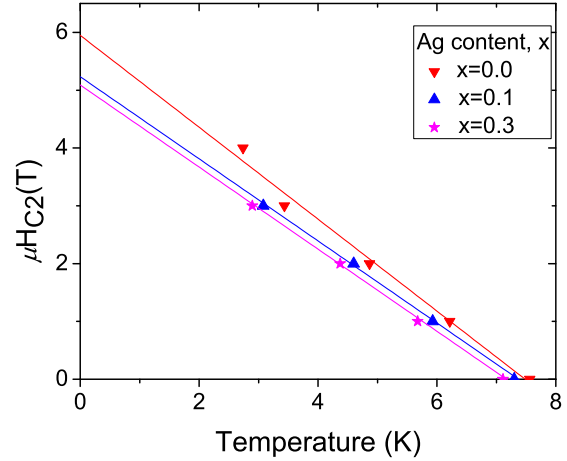


**Fig. 6** Upper critical field as a function of temperature determined from magneto-resistance measurements of  $\text{Li}_2\text{Pd}_{3-x}\text{Ag}_x\text{B}$  ( $x=0.0$ , 0.1 and 0.3). The continuous lines are linear fit of data and its extrapolation to  $T = 0$  K gives the values of  $H_{c2}^{linear}(0)$

The obtained Pauli limit field,  $\mu_0 H^{Pauli} = \Delta_0 / \mu_B \sqrt{2}$  [29], takes values of 17.83 T ( $x=0.0$ ), 16.91 T ( $x=0.1$ ) and 17.77 T ( $x=0.3$ ). It is noteworthy, that these values are higher than the values obtained from the upper critical fields. Accordingly, if the upper critical field in a single crystal exceeds the Pauli limit this suggests and implies a substantial contribution from the spin-triplet component to the pairing amplitude, presumably because broken inversion symmetry [22]. However, in this study the Pauli limiting field is greater than the upper critical fields  $\mu_0 H_{c2}(0)^{WHH}$  and  $\mu_0 H_{c2}(0)^{linear}$ , suggesting that the Cooper pairs are in spin-singlet state. The upper critical fields values obtained from a linear

extrapolation and the WHH theory shows a decrease while increasing Ag substitution: As a result a increase in  $\xi_0$  values is obtained for the samples in study.

### 3.3 Specific heat

In the normal state, above the transition temperature, the specific heat data is well fitted by a sum of the electronic and lattice contribution [30]:

$$C_p = \gamma T + \beta T^3. \quad (3)$$

A linear fit to  $C_p/T$  vs  $T^2$  plot of the  $\text{Li}_2\text{Pd}_{3-x}\text{Ag}_x\text{B}$  with  $x=0.0, 0.1$  and  $0.3$  are shown in Figure 7 yielding the Sommerfeld coefficient  $\gamma$  and the Debye constant  $\beta$ . For the sample without Ag the value of  $\gamma$  is  $1.26 \text{ mJ/molK}^2$ , this value is a little bit higher than the reported previously, which varies from  $8.3$  to  $9.8 \text{ mJ/molK}^2$  [31,32]. From the value of  $\beta$  we estimate the Debye temperature using the relation

$$\theta_D = \left( \frac{12n\pi^4 R}{5\beta} \right)^{\frac{1}{3}} \quad (4)$$

where  $n$  is the number of atoms per formula unit. The value of  $\theta_D$  for the  $\text{Li}_2\text{Pd}_3\text{B}$  sample is  $207.8 \text{ K}$ , which agrees with the reported values of  $221 \text{ K}$  [31] and  $202 \text{ K}$  [33]. On the other hand using the experimental Sommerfeld constant  $\gamma$ , the electronic density of states at Fermi level  $N(E_F)$  can be deduced using the formula:

$$N(E_F) = \frac{3\gamma}{\pi^2 k_B^2 N_A}. \quad (5)$$

$k_B$  is the Boltzmann's constant and  $N_A$  the Avogadro's number. The parameters obtained are shown in Table 2. It can be seen that there is a non-monotonic variation of  $N(E_F)$  and  $\gamma$  as the concentration of Ag is increased. This may be due to the impurity of  $\text{B}_2\text{Pd}_5$  on the sample  $\text{Li}_2\text{Pd}_{2.7}\text{Ag}_{0.3}\text{B}$ .

In the inset of Figure 7,  $C_p/T$  vs  $T$  is plotted detail of the specific heat jump at the thermodynamic transition.

From the critical temperature  $T_c$  and Debye temperature  $\theta_D$ , we can estimate the electron-phonon coupling constant  $\lambda_{e-ph}$  with the Mc Millan's relation [34] given below

$$\lambda_{e-ph} = \frac{1.04 + \mu^* \ln(\theta_D/1.45T_c)}{(1 - 0.62\mu^*) \ln(\theta_D/1.45T_c) - 1.04} \quad (6)$$

where  $\mu^*$  represents the screened repulsive Coulomb potential, usually in the range  $0.1$ - $0.15$ , in this work we used the value of  $0.13$ . This value is normally used for intermetallic superconductors [31,34]. The values of  $\lambda_{e-ph}$  obtained in this study range from  $0.84$  and  $0.81$

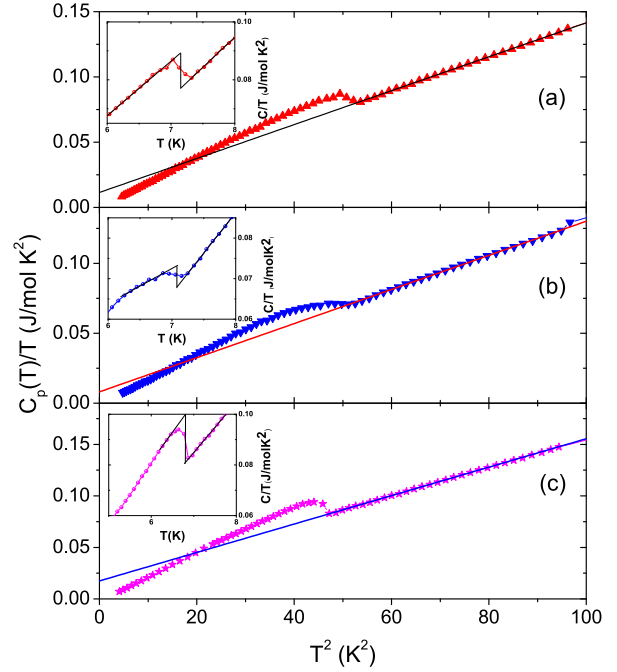


**Fig. 7**  $C_p/T$  versus  $T^2$  curves of  $\text{Li}_2\text{Pd}_{3-x}\text{Ag}_x\text{B}$ ; (a)  $x=0.0$ , (b)  $x=0.1$  and (c)  $x=0.3$ . The solid line represents a linear fit to the specific heat in the normal state. The inset shows  $C_p/T$  versus  $T$  to determine the specific heat jump at the superconducting transition.

for different contents of Ag. The value reported for the  $\text{Li}_2\text{Pd}_3\text{B}$  compound is  $\lambda_{e-ph} = 1.09$  [31], which is higher than that obtained in this work. The values of  $\lambda_{e-ph}$  are shown in Table 2 and allows to classify the system  $\text{Li}_2\text{Pd}_{3-x}\text{Ag}_x\text{B}$  with  $x=0.0, 0.1$  and  $0.3$  in a moderated coupled superconductor state.

At low temperatures the specific heat fit well to an exponential decay [35]:

$$C_p = C_0 + A \exp\left(\frac{-\Delta_0}{k_B T}\right), \quad (7)$$

where  $C_0$  is assumed as background of  $C_p$ . In order to determine the superconducting energy gap,  $2\Delta_0$ , the  $C_p(T)$  data were fitted with equation 7. The fit is shown as a continuous line in Figure 8. The obtained values of the superconducting gap,  $2\Delta_0$  and  $2\Delta_0/k_B T_c$  for the samples under study are shown in Table 2.

Several values of the superconducting energy gap of  $\text{Li}_2\text{Pd}_3\text{B}$  have been reported, from  $2.55$  to  $3.2 \text{ meV}$  [31, 32,36], the value of  $2\Delta_0 = 2.92 \text{ meV}$ , obtained in this work, agrees with these values. The values of  $2\Delta_0/k_B T_c$  obtained in this work increase from  $4.60$  for  $x=0.0$  to  $5.03$  for  $x=0.3$ , these values are higher than the value predicted by BCS,  $2\Delta_0/k_B T_c = 3.52$ , and to the reported value of  $3.94$  [31]. Our results indicate that the



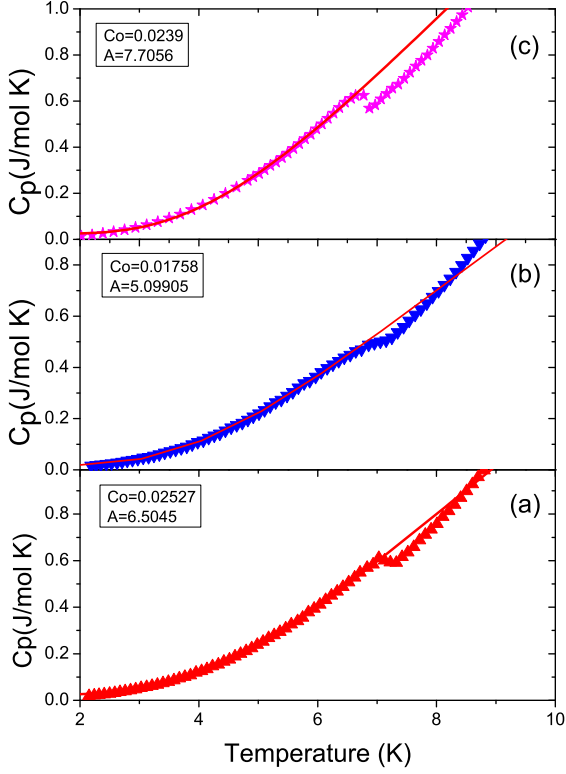


**Fig. 8**  $C_p$  versus  $T$  curves of  $\text{Li}_2\text{Pd}_{3-x}\text{Ag}_x\text{B}$ ; (a)  $x=0.0$ , (b)  $x=0.1$  and (c)  $x=0.3$ . The solid line represents a linear fit to equation 7.

system  $\text{Li}_2\text{Pd}_{3-x}\text{Ag}_x\text{B}$  with  $x=0.0, 0.1$  and  $0.3$  is a superconducting system with strong electron-phonon coupling.

The specific heat jump at  $T_c$ ,  $\Delta C/\gamma T_c$  determined from  $C_p(T)$  data are lower than the BCS predicted value, 1.43, and to the reported values in  $\text{Li}_2\text{Pd}_3\text{B}$  [31, 32, 36] that varies from 1.6 to 2. Differences of  $\Delta C/\gamma T_c$  between different reports may be due to the difficulties in achieving the stoichiometry of Li and disorder in the samples.

We compare the results obtained in this work with the other published  $\text{Li}_2\text{Pd}_{3-x}\text{Cu}_x\text{B}$  with  $x=0.0, 0.1$  and  $0.2$ , where the lattice parameter decreases,  $a$ , as the nominal concentration of Cu increases. It is clear that the substitution of Pd with Ag and Cu generates an internal pressure in the unit cell and therefore a decrement of  $T_c$ , which can be related with a decrease in the  $2\Delta(0)$ .

**Table 2** Parameters obtained from the specific heat of the system  $\text{Li}_2\text{Pd}_{3-x}\text{Ag}_x\text{B}$  ( $x=0.0, 0.1$  and  $0.3$ ); Sommerfeld coefficient  $\gamma$ , density of states at Fermi level  $N(E_F)$ , Debye constant  $\beta$ , Debye temperature  $\theta_D$ , transition temperature  $T_c$ , specific heat jump at  $T_c$  divided by  $\gamma T_c$   $\Delta C/\gamma T_c$ , electron-phonon coupling constant  $\lambda_{e-ph}$ , superconducting energy gap  $2\Delta(0)$  and the ratio  $2\Delta/k_B T_c$ .

$x$	0.0	0.1	0.3
$\gamma$ (mJ/mol K <sup>2</sup> )	$11.26 \pm 0.31$	$8.11 \pm 0.37$	$17.48 \pm 0.26$
$N(E_F)$ (eV <sup>-1</sup> )	$2.43 \pm 0.065$	$1.72 \pm 0.078$	$3.70 \pm 0.055$
$\beta$ (mJ/mol K <sup>4</sup> )	$1.3 \pm 0.004$	$1.22 \pm 0.005$	$1.38 \pm 0.004$
$\theta_D$ (K)	208	212	204
$T_c$ (K)	7.36	6.89	6.72
$\Delta C/\gamma T_c$	$0.96 \pm 0.03$	$1.14 \pm 0.05$	$0.89 \pm 0.01$
$\lambda_{e-f}$	0.84	0.81	0.82
$2\Delta(0)$ (meV)	$2.92 \pm 0.03$	$2.77 \pm 0.02$	$2.91 \pm 0.04$
$2\Delta(0)/k_B T_c$	$4.60 \pm 0.03$	$4.67 \pm 0.03$	$5.03 \pm 0.07$

## 4 Conclusions

In this work we reported the synthesis of three polycrystalline samples of  $\text{Li}_2\text{Pd}_{3-x}\text{Ag}_x\text{B}$  with compositions:  $x=0.0, 0.1$  and  $0.3$  prepared by arc melting technique. Rietveld analysis of the X-ray diffraction patterns shows an increase in lattice parameters as Ag content increases. Magnetization, electrical transport and specific heat measurements confirms that the superconducting transition temperature,  $T_c$ , decreases as the content of Ag is increased. The upper critical fields  $\mu_0 H_{c2}^{WH}(0)$  and  $\mu_0 H_{c2}^{linear}(0)$  are lower than the Pauli limiting field which suggests that the pairing is in a spin-singlet state. The behavior of the low-temperature specific heat, allows to classify this system as a superconductors with an isotropic energy gap as a conventional BCS superconductor, where the ratio,  $2\Delta_0/k_B T_c$ , values are indicative of strong coupling, contrary to the determined in other studies already published. We noted that Ag substitution decreases the electron  $N(E_F)$ , observed in the decreasing of the energy gap. For the two compounds with Ag the evidence is not so clear because we found small impurities. However in the most pure sample the effect is quite clear.

## Acknowledgments

We acknowledge to DGAPA-UNAM IT100217, M. C, A. Bobadilla for helium supply, and also to A. Lopez, Alan Dierick Ortega Gutiérrez and A. Pompa-Garcia for help in computing details. A. A. Castro thanks CONACYT, for the support through the Posdoctoral Scholarship and C. González for help in computing details.

## Conflict of interest

The authors declare that they have not conflict of interest.

## References

1. H. Hosono, A. Yamamoto, H. Hiramatsu, Y. Ma, *Materials Today* **21**(3), 278 (2018)
2. X. Liu, L. Zhao, S. He, J. He, D. Liu, D. Mou, B. Shen, Y. Hu, J. Huang, X.J. Zhou,
3. F.C. Hsu, J.Y. Luo, K.W. Yeh, T.K. Chen, T.W. Huang, P.M. Wu, Y.C. Lee, Y.L. Huang, Y.Y. Chu, D.C. Yan, M.K. Wu, **105**(38), 14262 (2008)
4. M.R. Koblishka, Y. Slimani, A. Koblishka-Veneva, T. Karwoth, X. Zeng, E. Hannachi, M. Murakami, *Materials* **13**(21) (2020)
5. E. Bauer, M. Sigrist, *Non-centrosymmetric Superconductors*, vol. 847 (Springer, Berlin, Heidelberg, 2012)
6. P.W. Anderson, *Phys. Rev. B* **30**, 4000 (1984)
7. V.K. Anand, A.D. Hillier, D.T. Adroja, A.M. Strydom, H. Michor, K.A. McEwen, B.D. Rainford, *Phys. Rev. B* **83**, 064522 (2011)
8. L.P. Gor'kov, E.I. Rashba, *Phys. Rev. Lett.* **87**, 037004 (2001)
9. P.A. Frigeri, D.F. Agterberg, A. Koga, M. Sigrist, *Phys. Rev. Lett.* **92**, 097001 (2004)
10. M. Sigrist, D. Agterberg, P. Frigeri, N. Hayashi, R. Kaur, A. Koga, I. Milat, K. Wakabayashi, Y. Yanase, *Journal of Magnetism and Magnetic Materials* **310**(2, Part 1), 536 (2007). *Proceedings of the 17th International Conference on Magnetism*
11. M. Smidman, M.B. Salamon, H.Q. Yuan, D.F. Agterberg, *Reports on Progress in Physics* **80**(3), 036501 (2017)
12. N. Kimura, K. Ito, K. Saitoh, Y. Umeda, H. Aoki, T. Terashima, *Phys. Rev. Lett.* **95**, 247004 (2005)
13. I. Sugitani, Y. Okuda, H. Shishido, T. Yamada, A. Thamizhavel, E. Yamamoto, T. D. Matsuda, Y. Haga, T. Takeuchi, R. Settai, Y. Ōnuki, *Journal of the Physical Society of Japan* **75**(4), 043703 (2006)
14. T. Akazawa, H. Hidaka, H. Kotegawa, T. C. Kobayashi, T. Fujiwara, E. Yamamoto, Y. Haga, R. Settai, Y. Ōnuki, *Journal of the Physical Society of Japan* **73**(11), 3129 (2004)
15. M. Yogi, Y. Kitaoka, S. Hashimoto, T. Yasuda, R. Settai, T.D. Matsuda, Y. Haga, Y. Ōnuki, P. Rogl, E. Bauer, *Phys. Rev. Lett.* **93**, 027003 (2004)
16. K. Izawa, Y. Kasahara, Y. Matsuda, K. Behnia, T. Yasuda, R. Settai, Y. Ōnuki, *Phys. Rev. Lett.* **94**, 197002 (2005)
17. K. Togano, P. Badica, Y. Nakamori, S. Orimo, H. Takeya, K. Hirata, *Phys. Rev. Lett.* **93**, 247004 (2004)
18. A. Castro, O. Olicón, R. Escamilla, F. Morales, *Solid State Communications* **255-256**, 11 (2017)
19. P. Badica, T. Kondo, K. Togano, *Journal of the Physical Society of Japan* **74**(3), 1014 (2005)
20. T. Klimczuk, Q. Xu, E. Morosan, J.D. Thompson, H.W. Zandbergen, R.J. Cava, *Phys. Rev. B* **74**, 220502 (2006)
21. T. Shiba, Y. Nohara, H. Aruga Katori, Y. Okamoto, Z. Hiroi, H. Takagi, *Journal of the Physical Society of Japan* **76**(7), 073708 (2007)
22. A.B. Karki, Y.M. Xiong, N. Haldolaarachchige, S. Stadler, I. Vekhter, P.W. Adams, D.P. Young, W.A. Phelan, J.Y. Chan, *Phys. Rev. B* **83**, 144525 (2011)
23. A. Mani, N. Gayathri, A. Bharathi, *Solid State Communications* **149**(23), 899 (2009)
24. M. Nishiyama, Y. Inada, G.Q. Zheng, *Phys. Rev. B* **71**, 220505 (2005)
25. L. Lutterotti, M. Bortolotti, G. Ischia, I. Lonardelli, H.R. Wenk, *Z. Kristallogr. Suppl.* **26**, 125 (2007)
26. L. Chen, L.R. Zhang, L.Y. Yao, Y.H. Fang, L. He, G.F. Wei, Z.P. Liu, *Energy Environ. Sci.* **12**, 3099 (2019)
27. N.R. Werthamer, E. Helfand, P.C. Hohenberg, *Phys. Rev.* **147**, 295 (1966)
28. P.K. Biswas, M.R. Lees, A.D. Hillier, R.I. Smith, W.G. Marshall, D.M. Paul, *Phys. Rev. B* **84**, 184529 (2011)
29. A.M. Clogston, *Phys. Rev. Lett.* **9**, 266 (1962)
30. A. Tari, *The Specific Heat of Matter at Low Temperatures* (Imperial College Press, 2003)
31. H. Takeya, K. Hirata, K. Yamaura, K. Togano, M. El Massalami, R. Rapp, F.A. Chaves, B. Ouladdiaf, *Phys. Rev. B* **72**, 104506 (2005)
32. H. Takeya, M. ElMassalami, S. Kasahara, K. Hirata, *Phys. Rev. B* **76**, 104506 (2007)
33. H. Takeya, S. Kasahara, M. El Massalami, K. Hirata, K. Togano, *Physica C: Superconductivity and its Applications* **463-465**, 111 (2007). *Proceedings of the 19th International Symposium on Superconductivity (ISS 2006)*
34. W.L. McMillan, *Phys. Rev.* **167**, 331 (1968)
35. R. Escudero, R.E. López-Romero, *Solid State Communications* **220**, 21 (2015)
36. H. Takeya, S. Kasahara, M. El Massalami, T. Mochiku, K. Hirata, K. Togano, *Physica B: Condensed Matter* **403**(5), 1078 (2008)